PHYSICAL REVIEW D **84,** 114505 (2011)

$D \to \pi, l\nu$ semileptonic decays, $|V_{cd}|$ and second row unitarity from lattice QCD

Heechang Na,[1] Christine T. H. Davies,[2] Eduardo Follana,[3] Jonna Koponen,[2]
G. Peter Lepage,[4] and Junko Shigemitsu[1]

(HPQCD Collaboration)

[1]*Department of Physics, The Ohio State University, Columbus, Ohio 43210, USA*
[2]*SUPA, School of Physics and Astronomy, University of Glasgow, Glasgow, G12 8QQ, United Kingdom*
[3]*Departamento de Fisica Teorica, Universidad de Zaragoza, E-50009 Zaragoza, Spain*
[4]*Laboratory of Elementary Particle Physics, Cornell University, Ithaca, New York 14853, USA*
(Received 9 September 2011; published 27 December 2011)

We present a new calculation of the $D \to \pi, l\nu$ semileptonic form factor $f_+^{D\to\pi}(q^2)$ at $q^2 = 0$ based on "highly improved staggered quark" charm and light valence quarks on MILC $N_f = 2 + 1$ lattices. Using methods developed recently for HPQCD's study of $D \to K$, $l\nu$ decays, we find $f_+^{D\to\pi}(0) = 0.666(29)$. This signifies a better than factor 2 improvement in errors for this quantity compared to previous calculations. Combining the new result with CLEO-c branching fraction data, we extract the Cabibbo-Kobayashi-Maskawa matrix element $|V_{cd}| = 0.225(6)_{\rm exp}(10)_{\rm lat}$, where the first error comes from experiment and the second from theory. With a total error of ~5.3% the accuracy of the direct determination of $|V_{cd}|$ from D semileptonic decays has become comparable to (and in good agreement with) that from neutrino scattering. We also check for second row unitarity using this new $|V_{cd}|$, HPQCD's earlier $|V_{cs}|$, and $|V_{cb}|$ from the Fermilab Lattice and MILC collaborations. We find $|V_{cd}|^2 + |V_{cs}|^2 + |V_{cb}|^2 = 0.976(50)$, improving on the current PDG2010 value.

DOI: 10.1103/PhysRevD.84.114505 PACS numbers: 12.38.Gc, 13.20.Fc

I. INTRODUCTION

The Cabibbo-Kobayashi-Maskawa (CKM) matrix provides particle physicists with a wealth of opportunities to carry out precision tests of the standard model (SM) and look for new physics. On the one hand, each matrix element can be determined in several ways, employing different experimental and theory inputs, and the results compared with each other. Three generation unitarity can also be examined to see how well $\hat{V}_{\rm CKM} \times \hat{V}_{\rm CKM}^\dagger = \hat{I}$ is satisfied. This leads to tests such as first, second, or third row/column unitarity. It also gives rise to the important "unitarity triangle" (UT) relation $V_{ud} * V_{ub}^* + V_{cd} * V_{cb}^* + V_{td} * V_{tb}^* = 0$. Consistency checks of the sides and angles of the UT have been the focus of much of the experimental and theoretical effort in flavor physics in recent years. Lattice QCD is playing an increasingly important role in CKM physics [1]. For instance, lattice calculations of the kaon semileptonic form factor $f_+^{K\to\pi}(0)$ [2,3] and the decay constant f_K (or f_K/f_π) [4–8] have contributed to precision determinations of $|V_{us}|$ and first row unitarity tests [9].

The HPQCD Collaboration recently published a new lattice calculation of the $D \to K$, $l\nu$ semileptonic decay form factor $f_+^{D\to K}(q^2)$ at $q^2 = 0$ [10] which significantly reduced the error on this quantity compared to previous theory results. This led to a very precise determination of the CKM matrix element $|V_{cs}|$. Features in the HPQCD work that made this improvement possible include the use of a relativistic quark action, the "highly improved staggered quark" (HISQ) action [11], to simulate both light and charm quarks, and better data analysis tools. We also extended standard lattice QCD approaches of combining continuum and chiral extrapolations to semileptonic decays. Capitalizing on these developments, we turn here in this article to $D \to \pi, l\nu$ semileptonic decays. We focus on extracting the CKM matrix element $|V_{cd}|$ by combining theory results for $f_+^{D\to\pi}(0)$ with experimental input from CLEO-c [12]. The first unquenched lattice studies of D semileptonic decays were carried out several years ago by the Fermilab Lattice and MILC collaborations [13]. In that work lattice gauge theory was able to predict the shape of $f_+(q^2)$ prior to subsequent confirmation by experiment. The theory errors for $f_+^{D\to\pi}(0)$ in [13] were ~10%, and this has remained the dominant error in determinations of $|V_{cd}|$ from D semileptonic decays. More accurate determinations have come from neutrino scattering experiments so that the current PDG2010 [14] quotes $|V_{cd}|$ from neutrino charm production with an error of about ~5%. With the new lattice calculations described in this article, the accuracy of $|V_{cd}|$ from D semileptonic decays is approaching that from neutrino scattering and this provides an important consistency check. We find

$$|V_{cd}| = 0.225(6)_{\rm exp}(10)_{\rm lat}, \tag{1}$$

where the first error is from experiment [12] and the second is the theory error from the lattice QCD calculation presented here. Equation (1) is in excellent agreement

TABLE I. The MILC $N_f = 2 + 1$ ensembles used in the $D \to \pi$ semileptonic project. The fourth column gives the valence HISQ light and charm quark masses in lattice units. $N_{\rm conf}$ is the number of configurations and $N_{\rm tsrc}$ the number of time sources used for each configuration.

Set	r_1/a	m_l(sea)/m_s(sea)	$am_{\rm valence}$	$N_{\rm conf}$	$N_{\rm tsrc}$	$L^3 \times N_t$
C1	2.647	0.005/0.050	0.0070	1200	2	$24^3 \times 64$
			0.6207	1200	2	
C2	2.618	0.010/0.050	0.0123	1200	2	$20^3 \times 64$
			0.6300	1200	2	
C3	2.644	0.020/0.050	0.0246	600	2	$20^3 \times 64$
			0.6235	600	2	
F1	3.699	0.0062/0.031	0.00674	1200	4	$28^3 \times 96$
			0.4130	1200	4	
F2	3.712	0.0124/0.031	0.0135	600	4	$28^3 \times 96$
			0.4120	600	4	

with the PDG value based on neutrino scattering of $|V_{cd}| = 0.230(11)$.

In the rest of this article we describe how the result of Eq. (1) was obtained. We work with HISQ valence charm and light quarks on the MILC AsqTad $N_f = 2 + 1$ coarse ($a \sim 0.12$ fm) and fine ($a \sim 0.09$ fm) lattices. Table I lists the five MILC [15] ensembles employed in this work and some simulation parameters. Compared to [10] we have doubled the statistics on ensembles C1, C2, and F1. The valence charm and light bare quark masses are the same as in [10], with the former tuned to the η_c mass and the latter chosen such that the ratio of $m_{\rm light}$ to the physical strange quark mass is approximately the same for valence and sea quarks. In the next section we summarize the formulas for hadronic matrix elements necessary to extract $f_+^{D\to\pi}(0)$ and explain how they are related to three- and two-point correlators evaluated numerically on the lattice. These relations are the same as those described in Ref. [10] so we will be brief. In Sec. III we describe our data analysis and fitting procedures. We employ Bayesian fitting methods and carry out multiexponential fits to several three-point and two-point correlators at the same time. Section IV discusses chiral and continuum extrapolations of lattice results to the physical limit. We apply the modified z-expansion method developed for $D \to K$ semileptonic form factors in [10]. Section V presents our results for $f_+^{D\to\pi}(0)$ and $|V_{cd}|$ and comparisons with other determinations of these quantities. Section VI gives a brief summary, and we also include a second row unitarity test with all theory inputs coming from lattice QCD.

II. RELEVANT MATRIX ELEMENTS

The most efficient way to calculate $f_+(q^2)$ at $q^2 = 0$ is to focus on the scalar form factor $f_0(q^2)$ and use the kinematic identity $f_+(0) = f_0(0)$. The scalar form factor can be determined from the matrix element of the scalar current $S = \bar{\Psi}_q \Psi_c$ between the D meson and pion states.

$$f_0^{D\to\pi}(q^2) = \frac{(m_{0c} - m_{0l})\langle\pi|S|D\rangle}{M_D^2 - M_\pi^2}. \tag{2}$$

The combination in the numerator of Eq. (2) does not get renormalized. The use of absolutely normalized currents is one of the reasons why we are able to significantly reduce errors in our D semileptonic scalar form factor calculations, both here and in [10].

Our goal is to determine the hadronic matrix element $\langle\pi|S|D\rangle$ in Eq. (2) via numerical simulations. The starting point is the three-point correlator,

$$C^{\rm 3pnt}(t_0, t, T, \vec{p}_\pi) = \frac{1}{L^3}\sum_{\vec{x}}\sum_{\vec{y}}\sum_{\vec{z}} e^{i\vec{p}_\pi\cdot(\vec{z}-\vec{x})}, \\ \langle\Phi_\pi(\vec{x}, t_0)\tilde{S}(\vec{z}, t)\Phi_D^\dagger(\vec{y}, t_0 - T)\rangle. \tag{3}$$

In Eq. (3) the interpolating operator $\Phi_D^\dagger$ creates a D meson at time slice $t_0 - T$. At time t ($t_0 \geq t \geq t_0 - T$) the scalar current S converts the c quark inside the D into a light quark and also inserts momentum $\vec{p}_\pi$. The resulting pion then propagates to time slice t_0 where it is annihilated by Φ_π. In addition to the three-point correlator, one needs the pion and D meson two-point correlators,

$$C_D^{\rm 2pnt}(t, t_0) = \frac{1}{L^3}\sum_{\vec{x}}\sum_{\vec{y}}\langle\Phi_D(\vec{y}, t)\Phi_D^\dagger(\vec{x}, t_0)\rangle \tag{4}$$

and

$$C_\pi^{\rm 2pnt}(t, t_0; \vec{p}_\pi) = \frac{1}{L^3}\sum_{\vec{x}}\sum_{\vec{y}} e^{i\vec{p}_\pi\cdot(\vec{x}-\vec{y})}\langle\Phi_\pi(\vec{y}, t)\Phi_\pi^\dagger(\vec{x}, t_0)\rangle. \tag{5}$$

Details on how the above three- and two-point correlators can be expressed in terms of single component staggered quark propagators are given in Sec. IV of Ref. [10] and will not be repeated here. There we also show how the sums $\sum_{\vec{x}}$ in Eqs. (3)–(5) can be carried out using U(1) random wall sources.

The meson creation operators $\Phi_D^\dagger$ and $\Phi_\pi^\dagger$ create not only the ground state D and pion we are interested in, but also an arbitrary number of excited states with the same quantum numbers. Hence the t dependence of the two- and three-point correlators is complicated especially for staggered quarks. For two-point correlators it is given by

$$C_D^{\rm 2pnt}(t) = \sum_{j=0}^{N_D-1} b_j^D(e^{-E_j^D t} + e^{-E_j^D(N_t - t)}) \\ + \sum_{k=0}^{N'_D-1} d_k^D(-1)^t(e^{-E_k'^D t} + e^{-E_k'^D(N_t - t)}), \tag{6}$$

and similarly for $C_\pi^{\rm 2pnt}(t)$, except that there is no opposite parity terms for zero momentum. For three-point correlators one has

$$C^{3\mathrm{pnt}}(t,T) = \sum_{j=0}^{N_\pi-1}\sum_{k=0}^{N_D-1} A_{jk} e^{-E_j^\pi t} e^{-E_k^D (T-t)} + \sum_{j=0}^{N_\pi-1}\sum_{k=0}^{N'_D-1} B_{jk} e^{-E_j^\pi t} e^{-E_k'^D (T-t)} (-1)^{(T-t)} + \sum_{j=0}^{N'_\pi-1}\sum_{k=0}^{N_D-1} C_{jk} e^{-E_j'^\pi t} e^{-E_k^D (T-t)} (-1)^t + \sum_{j=0}^{N'_\pi-1}\sum_{k=0}^{N'_D-1} D_{jk} e^{-E_j'^\pi t} e^{-E_k'^D (T-t)} (-1)^t (-1)^{(T-t)}. \quad (7)$$

We are interested in the ground state contributions with amplitudes

$$b_0^D \equiv \frac{|\langle \Phi_D | D \rangle|^2}{2M_D a^3}, \quad (8)$$

$$b_0^\pi \equiv \frac{|\langle \Phi_\pi | \pi \rangle|^2}{2E_\pi a^3}, \quad (9)$$

and

$$A_{00} \equiv \frac{\langle \Phi_\pi | \pi \rangle \langle \pi | S | D \rangle \langle D | \Phi_D \rangle}{(2E_\pi a^3)(2M_D a^3)} a^3. \quad (10)$$

So the hadronic matrix element $\langle \pi | S | D \rangle$ that enters into the formula for $f_0^{D\to\pi}(0)$ in (2) is given by

$$\langle \pi | S | D \rangle = 2\sqrt{M_D E_\pi} \frac{A_{00}}{\sqrt{b_0^\pi b_0^D}}. \quad (11)$$

We have accumulated simulation data for zero momentum D correlators and for pion correlators with momenta $\frac{2\pi}{L}(0,0,0)$, $\frac{2\pi}{L}(1,0,0)$, $\frac{2\pi}{L}(1,1,0)$, and $\frac{2\pi}{L}(1,1,1)$. The corresponding three-point correlators were calculated for $T = 15$, 16 on the coarse ensembles and for $T = 19$, 20, 23 on the fine ensembles. In the next section we describe how the combination on the right-hand side of (11) is obtained from three- and two-point correlators.

III. FITS AND DATA ANALYSIS

Extracting energies and amplitudes from numerical data on two- and three-point correlators is one of the more challenging but, at the same time, very important aspects of lattice calculations. For the past decade the HPQCD Collaboration has been employing fitting methods based on Bayesian statistics and involving multiexponential fits [16]. For instance, in order to obtain the ground state energy and amplitude from a two-point correlator, we drop the first 1–4 time slices and then fit to the form of Eq. (6) for several values of $N \equiv N_D$ (or N_π) and N'. One continues to increase the number of exponentials until the fit results for E_0 and b_0, including their errors and the chi-squared per degree of freedom of the fit, have stabilized. Figure 1 shows an example of aE_π versus $N_{\mathrm{exp}} = N_\pi$ for momentum $\frac{2\pi}{L}(1,1,1)$ with $N'_\pi = N_\pi$. One sees that fits have stabilized after $N_{\mathrm{exp}} = 3$. It should be noted that as one increases the number of exponentials and with it the number of fit parameters, the number of data points grows as well. Each new fit parameter adds another prior term, i.e. additional data, to the fit function, and the number of data points minus the number of fit parameters remains constant [16].

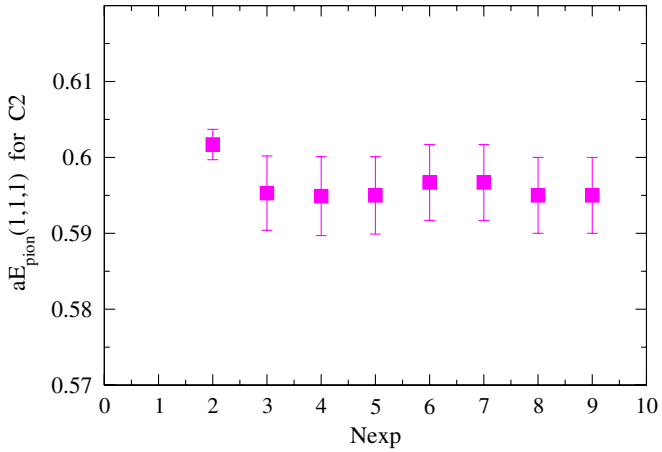

FIG. 1 (color online). Ground state pion energy in lattice units for momentum $\frac{2\pi}{L}(1,1,1)$ versus the number of exponentials in the fit.

The combination $\frac{A_{00}}{\sqrt{b_0^\pi b_0^D}}$ is obtained from simultaneous fits to $C_D^{2\mathrm{pnt}}(t)$, $C_\pi^{2\mathrm{pnt}}(t)$, and $C^{3\mathrm{pnt}}(t,T)$ for 2 (or 3) T values.

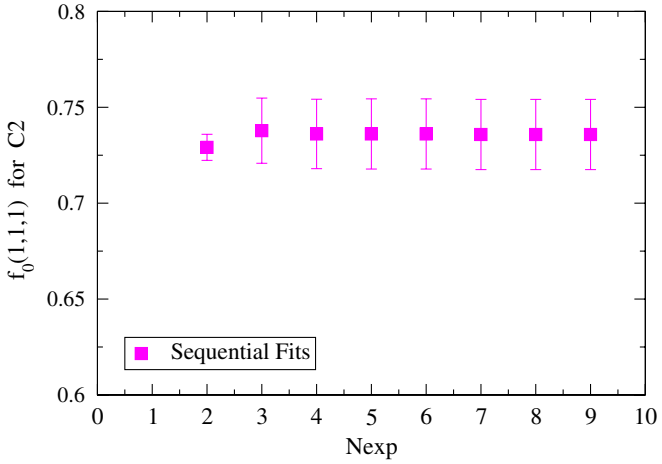

FIG. 2 (color online). The form factor $f_0(q^2)$ for pion momentum $\frac{2\pi}{L}(1,1,1)$ from simultaneous fits to two- and three-point correlators versus $N_{\mathrm{exp}} = N_D = N'_D = N_\pi = N'_\pi$. The sequential fitting method was employed to go from one N_{exp} value to the next. In this method the fit results from the N_{exp} exponential fit are inserted as initial conditions for the subsequent $[N_{\mathrm{exp}} + 1]$ exponential fit.

TABLE II. Results for $f_0(\vec{p}_\pi)$ for each ensemble.

Set	$f_0(0,0,0)$	$f_0(1,0,0)$	$f_0(1,1,0)$	$f_0(1,1,1)$
C1	1.1557(74)	0.9155(93)	0.8119(68)	0.7384(209)
C2	1.1014(38)	0.8700(59)	0.7801(43)	0.7315(87)
C3	1.0398(28)	0.8787(36)	0.7922(31)	0.7326(66)
F1	1.1053(29)	0.8652(52)	0.7586(53)	0.7112(108)
F2	1.0443(28)	0.8613(31)	0.7645(53)	0.7097(70)

In order to be able to include a large number of exponentials in these complicated fits, we proceed as follows. We set $N_\pi = N'_\pi = N_D = N'_D \equiv N_{\rm exp}$ and start out with a small value, $N_{\rm exp} = 2$ or $N_{\rm exp} = 3$. The fit results are then inserted as initial conditions for the subsequent $N_{\rm exp} + 1$ exponential fit. This procedure is repeated until one has completed multiexponential fits with $N_{\rm exp}$ much larger than 2. Figure 2 shows results for $f_0(q^2)$ on ensemble C2 at pion momentum $\frac{2\pi}{L}(1,1,1)$ versus $N_{\rm exp}$ using this "sequential fitting" procedure. One sees that, similar to in Fig. 1, fit results have stabilized for $N_{\rm exp} > 3$ [17].

In ongoing work we are investigating further methods to deal with complicated fits with a large number of parameters, in particular, fits to collections of sums of exponentials [18]. For the calculations of this article, however, we have found that the "sequential fitting" method described above works well for all our data [19]. We are even able to fit data on a given ensemble for all four pion momenta simultaneously, and this allows us to obtain correlations between form factor results at different q^2. These simultaneous fit results for $f_0(\vec{p}_\pi)$ are given in Table II for several pion momenta $\vec{p}_\pi$ (the latter in units of $\frac{2\pi}{L}$).

IV. CHIRAL AND CONTINUUM EXTRAPOLATION

The next step is to extrapolate the data of Table II to the chiral/continuum limit. We do so using the "modified z-expansion fit" developed in [10]. The scalar form factor is parametrized as

$$f_0(q^2) = \frac{1}{P(q^2)\Phi_0}(a_0 D_0 + a_1 D_1 z + a_2 D_2 z^2)(1 + b_1(aE_\pi)^2 + b_2(aE_\pi)^4), \tag{12}$$

with

$$D_i = 1 + c_1^i x_l + c_2^i x_l \log(x_l) + d_i(am_c)^2 + e_i(am_c)^4 + f_i(\tfrac{1}{2}\delta M_\pi^2 + \delta M_K^2), \tag{13}$$

$$x_l = \frac{M_\pi^2}{(4\pi f_\pi)^2}, \tag{14}$$

$$\delta M_\pi^2 = \frac{1}{(4\pi f_\pi)^2}((M_\pi^{\rm sea})^2 - (M_\pi^{\rm valence})^2), \tag{15}$$

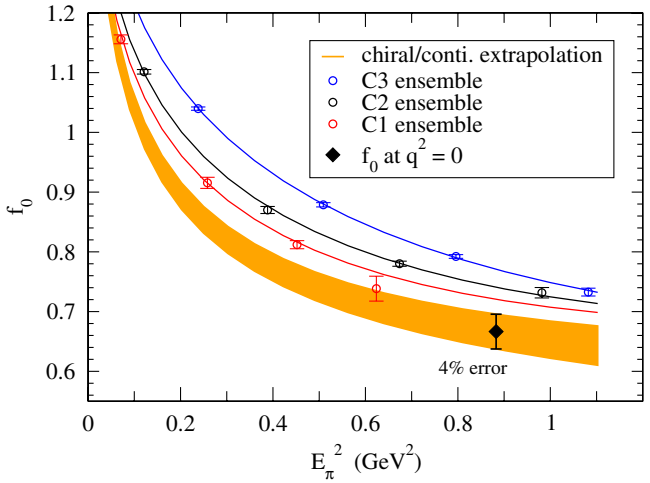

FIG. 3 (color online). Chiral/continuum extrapolation of $f_0^{D\to\pi}$ versus E_π^2. The data points are from the coarse ensembles (C1, C2, and C3). The three individual curves and the extrapolated band are from a fit to all five ensembles.

$$\delta M_K^2 = \frac{1}{(4\pi f_\pi)^2}((M_K^{\rm sea})^2 - (M_K^{\rm valence})^2). \tag{16}$$

The kinematic variable z is defined as [20–22]

$$z(q^2, t_0) = \frac{\sqrt{t_+ - q^2} - \sqrt{t_+ - t_0}}{\sqrt{t_+ - q^2} + \sqrt{t_+ - t_0}}, \tag{17}$$

with t_0 a free parameter (which we set equal to 1.95 GeV^2) and $t_\pm = (M_D \pm M_\pi)^2$. We take Φ_0 from [21] and set $P(q^2) = 1$, where the latter relation reflects the absence of subthreshold poles in the scalar channel.

We show results of fits to the form of Eq. (12) in Figs. 3 and 4. We plot separately the coarse and fine data points in order to be able to better distinguish individual curves. However, the fit was done simultaneously to all the data in Table II, coarse and fine. The $\chi^2/{\rm dof} = 0.85$ for this fit.

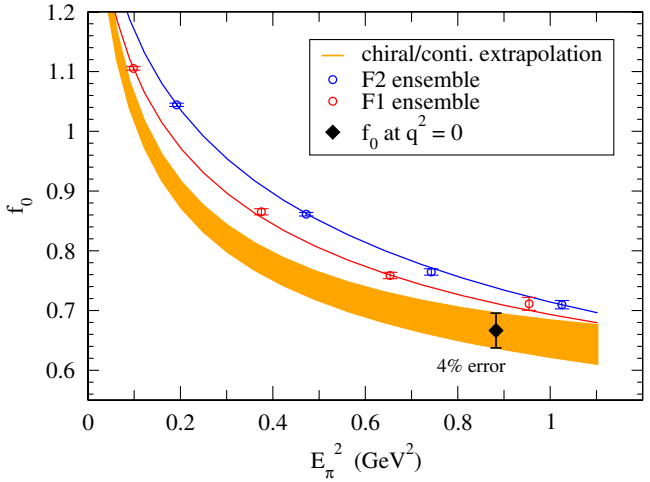

FIG. 4 (color online). Same as for Fig. 3 showing, however, the fine data points.

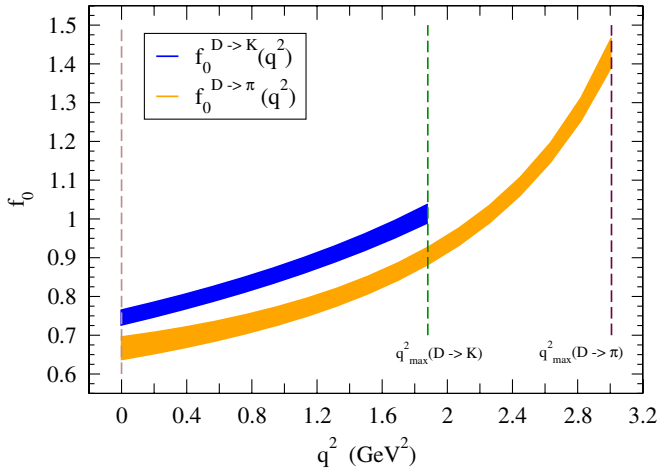

FIG. 5 (color online). $f_0^{D\to K}(q^2)$ and $f_0^{D\to\pi}(q^2)$ versus q^2 in the physical limit.

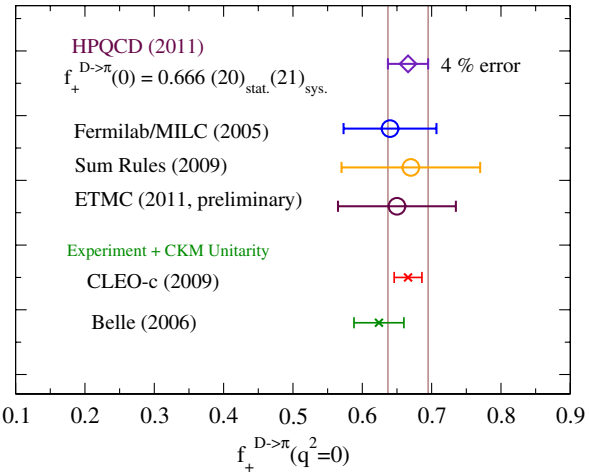

FIG. 6 (color online). The $D \to \pi$ form factor $f_+^{D\to\pi}(0)$ from this work and comparisons with other determinations [12,13,24–26].

In Fig. 5 we show both $f_0^{D\to K}(q^2)$ (results from [10]) and $f_0^{D\to\pi}(q^2)$ versus q^2 in the physical region $0 \le q^2 \le q^2_{\rm max} = (M_D - M_{\pi(K)})^2$. Note that we consider the correlations between the momenta in the fits which we did not consider in [10]. However, we find that including or excluding correlations in our chiral/continuum extrapolations has a minimal effect on $f_0^{D\to\pi}(0)$ at the physical point, namely, a $\sim 0.04\sigma$ shift in the central value and a $\sim 0.02\sigma$ change in the error.

The motivation for the "modified z-expansion fit" is explained in more detail in [10]. Form factors at $q^2 = 0$ are needed to extract the CKM matrix elements $|V_{cd}|$ or $|V_{cs}|$. The pion energy approaches 1 GeV in this kinematic region and so chiral perturbation theory (ChPT) might cease to be valid. The z expansion, on the other hand, is applicable throughout the physical kinematic region, and our new "modified z expansion" allows for the expansion coefficients to be mass and lattice spacing dependent. We have checked that fits to Eq. (12) are stable with respect to adding further terms such as x_l^2, $(am_c)^6$, $(aE_\pi)^6$ or keeping just the c_1^i and c_2^i terms in Eq. (13) (the D_i's). Such changes in the fit ansatz led to minimal changes in both the central value and the error for $f_0(0)$ in the physical limit. We have also verified that traditional ChPT extrapolations (see Appendixes C and D of [10] and references therein for relevant ChPT formulas) lead to $f_+(0)$ in the physical limit, consistent with the z-expansion result and with comparable errors, however with worse χ^2/dof. In addition, we test the extrapolations to $q^2 = 0$ with the Becirevic-Kaidalov parametrization [23] to individual ensembles, and obtain almost the same results as with the z-expansion method.

V. RESULTS FOR $f_+^{D\to\pi}(0)$ AND $|V_{cd}|$ IN THE PHYSICAL LIMIT

Our final result for the $D \to \pi$ form factor at $q^2 = 0$ averaged over $D^0 \to \pi^-$ and $D^+ \to \pi^0$ is

$$f_+^{D\to\pi}(0) = 0.666(20)_{\rm stat}(21)_{\rm sys}, \tag{18}$$

where the first error is statistical and the second systematic. Figure 6 plots our new result together with other theory calculations [13,24,25] and experimental determinations [12,26] [the latter use CKM unitarity values for $|V_{cd}|$ to extract $f_+^{D\to\pi}(0)$].

The total error in our $f_+^{D\to\pi}(0)$ is 4.4%, signifying a better than factor 2 improvement over previous lattice determinations. The full error budget is given in Table III. The largest error is statistical followed by am_c and light quark mass dependence errors. All but the last two entries in Table III were obtained using the methods described in Ref. [27] and Appendix B of [10]. For instance, the "light quark dependence" errors come from the c_1^i and c_2^i terms in the fit ansatz Eq. (13), the "am_c corrections" from the d_i and e_i terms, etc.

Finite volume errors were estimated by calculating a pion tadpole integral both at finite and at infinite volume.

TABLE III. Error budget for $f_+^{D\to\pi}(0)$.

Type	Error (%)
Statistical	3.1
Scale (r_1 and r_1/a)	0.7
Expansion coeff. a_i	0.3
E_p	0.6
Light quark dependence	1.9
Sea quark dependence	0.6
am_c corrections	2.0
aE_π corrections	1.0
Finite volume	0.04
Charm mass tuning	0.05
Total	4.4%

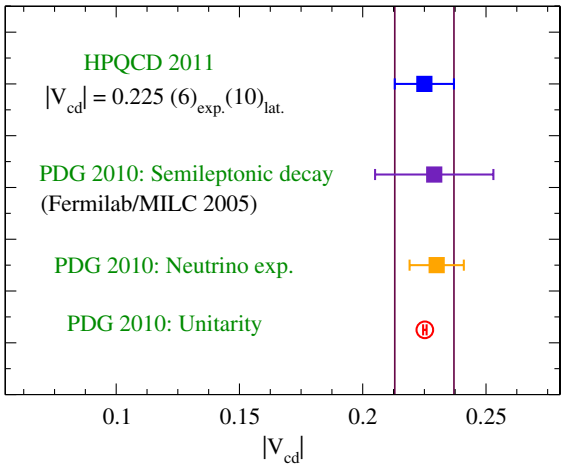

FIG. 7 (color online). Comparison of $|V_{cd}|$ from this work with values in PDG2010 [14].

The charm mass tuning error is taken to be the same as for $D \to K$, $l\nu$ for which calculations at two values of am_c were carried out explicitly to estimate this error. Effects from electromagnetism/isospin breaking and charm sea are expected to give a negligible contribution to the error budget compared to our other errors (see [10]). Also note that errors due to using different fermion actions on the sea and valence quarks are partially contained in the sea quark dependence errors and the discretization errors in Table III.

Finally, one can combine our result for $f_+^{D\to\pi}(0)$ with CLEO-c's measurement of $|V_{cd}| \times f_+^{D\to\pi}(0)$ [12] to extract a precision value for $|V_{cd}|$ from D semileptonic decays. This leads to the result quoted already in Eq. (1), which is shown in Fig. 7 together with values from PDG2010.

VI. SUMMARY

In this article we have presented a new calculation of the $D \to \pi$, $l\nu$ semileptonic form factor $f_+^{D\to\pi}(q^2)$ at $q^2 = 0$, with errors a factor of 2 better than in the past. This combined with the recent precision measurement of the branching fraction for this process by CLEO-c has allowed for an accurate determination of the CKM matrix element $|V_{cd}|$. Direct determination of $|V_{cd}|$ from D semileptonic decays is becoming competitive with that from neutrino scattering. The fact that these two very different processes lead to the same $|V_{cd}|$ is a nontrivial consistency check of the standard model.

Finally, using our values for $|V_{cd}|$ and $|V_{cs}|$ [10] plus the most recent $|V_{cb}|_{\text{excl}} = 0.0397(10)$ from the Fermilab Lattice and MILC collaborations [28], the most up-to-date test of second row unitary from lattice QCD becomes

$$|V_{cd}|^2 + |V_{cs}|^2 + |V_{cb}|^2 = 0.976(50). \qquad (19)$$

This improves on the PDG2010 value 1.101(74) [14].

In the future we will be reducing the largest errors in Table III by increasing statistics and simulating on finer lattices [29]. Calculations of the full q^2 dependence of $f_+^{D\to K}(q^2)$ and $f_+^{D\to\pi}(q^2)$ are also already underway [29]. Furthermore, we are working on updating HPQCD's result for the D meson decay constant f_D [5] and on carrying out an independent extraction of $|V_{cd}|$ from D leptonic decays [30].

ACKNOWLEDGMENTS

This work was supported by the DOE and NSF in the U.S., by STFC in the United Kingdom, and by MICINN and DGIID-DGA in Spain. We thank MILC for making their lattices available. Simulations were carried out on facilities of the USQCD Collaboration funded by the Office of Science of the DOE and at the Ohio Supercomputer Center.

APPENDIX: PRIORS AND PRIOR WIDTHS FOR TWO- AND THREE-POINT CORRELATORS

In this appendix we give sample priors and prior widths used in the fits of Sec. III (the reader is referred to Ref. [16] for definitions of these terms). All energies in Table IV are given in lattice units and are appropriate

TABLE IV. Sample priors and prior widths for two- and three-point correlator fits. Energies are in lattice units, and this example corresponds to priors used for ensemble C2. The notation is the same as in Eqs. (6) and (7).

	Prior	Prior width
E_0^D	1.16	0.58
$E_{j>0}^D - E_{j-1}^D$	0.36	0.36
$E_0'^D$	1.52	1.52
$E_{k>0}'^D - E_{k-1}'^D$	0.36	0.36
$\sqrt{b_j^D}$	0.01	0.5
$\sqrt{d_k^D}$	0.01	0.5
$E_0^\pi(000)$	0.21	0.11
$E_0^\pi(100)$	0.38	0.19
$E_0^\pi(110)$	0.49	0.25
$E_0^\pi(111)$	0.60	0.30
E_1^π(all mom) $- E_0^\pi$(all mom)	0.61	0.31
$E_{j>1}^\pi$(all mom) $- E_{j-1}^\pi$(all mom)	0.36	0.36
$E_0'^\pi(100)$	0.74	0.74
$E_0'^\pi(110)$	0.85	0.85
$E_0'^\pi(111)$	0.96	0.96
$E_{k>0}'^\pi(\text{mom} > 0) - E_{k-1}'^\pi(\text{mom} > 0)$	0.36	0.36
$\sqrt{b_j^\pi}$(all mom)	0.01	0.5
$\sqrt{d_k^\pi}(\text{mom} > 0)$	0.01	0.5
A_{jk}, B_{jk}, C_{jk}, D_{jk}	0.01	0.1

for ensemble C2. Numbers for other ensembles can be obtained by rescaling with corresponding lattice spacings. Prior widths for amplitudes are fixed based on exploratory initial fits. One might notice that these priors and prior widths are not exactly the same as the setting used in our previous work [10]. This is because we try to use more consistent priors and prior widths across all ensembles than Ref. [10]. We tested the current set against the previous set and found consistency between the two.

[1] For some recent reviews see R. Van de Water, Proc. Sci., LAT2009 (2009) 014; V. Lubicz, Proc. Sci., LAT2009 (2009) 013; J. Laiho, E. Lunghi, and R. Van de Water, Phys. Rev. D **81**, 034503 (2010); J. Shigemitsu, arXiv:1102.0716; J. Laiho, B. D. Pecjak, and C. Schwanda, arXiv:1107.3934.

[2] P. A. Boyle *et al.* (UKQCD/RBC Collaboration), Eur. Phys. J. C **69**, 159 (2010).

[3] V. Lubicz *et al.* (ETM Collaboration), Phys. Rev. D **80**, 111502 (2009).

[4] A. Bazavov *et al.* (MILC Collaboration), Proc. Sci., LATTICE2010 (2010) 074.

[5] E. Follana *et al.* (HPQCD/UKQCD Collaboration), Phys. Rev. Lett. **100**, 062002 (2008).

[6] S. Durr *et al.* (BMW Collaboration), Phys. Rev. D **81**, 054507 (2010).

[7] Y. Aoki *et al.* (RBC/UKQCD Collaboration), Phys. Rev. D **83**, 074508 (2011).

[8] B. Blossier *et al.* (ETM Collaboration), J. High Energy Phys. 07 (2009) 043.

[9] M. Antonelli *et al.* (FlaviaNet Working Group on Kaon Decays), Eur. Phys. J. C **69**, 399 (2010).

[10] H. Na *et al.* (HPQCD Collaboration), Phys. Rev. D **82**, 114506 (2010).

[11] E. Follana *et al.* (HPQCD/UKQCD Collaboration), Phys. Rev. D **75**, 054502 (2007).

[12] D. Besson *et al.* (CLEO Collaboration), Phys. Rev. D **80**, 032005 (2009).

[13] C. Aubin *et al.* (Fermilab Lattice and MILC Collaborations), Phys. Rev. Lett. **94**, 011601 (2005).

[14] K. Nakamura *et al.* (Particle Data Group), J. Phys. G **37**, 075021 (2010).

[15] C. Bernard *et al.* (MILC Collaboration), Phys. Rev. D **64**, 054506 (2001).

[16] G. P. Lepage *et al.* (HPQCD Collaboration), Nucl. Phys. B, Proc. Suppl. **106-107**, 12 (2002).

[17] For very complicated multiexponential fits, fit results can include fake low lying levels (with amplitudes that are consistent with zero) that distort ground state energies and fitting errors. Care is required to watch out for these spurious levels and make sure that fits that exhibit such levels are not trusted. The ''sequential fitting'' method adopted in this article has been very effective in preventing spurious levels from arising.

[18] K. Hornbostel *et al.* (HPQCD Collaboration) (to be published).

[19] In Ref. [10] the ''sequential fitting'' method was not employed. Instead, the number of exponentials in the three-point correlator ansatz was kept low, at 1 or 2, and only N exp in the two-point correlators increased as in Figs. 1 and 2. Good χ^2/dof were obtained in the simultaneous three- and two-point correlator fits, and the fits give consistent results for different T values. We took this as evidence that excited state contributions were suppressed in the three-point correlators compared to two-point correlators. By simplifying the fit ansatz in this manner, we were able to avoid spurious levels from appearing in [10].

[20] C. G. Boyd, B. Grinstein, and R. F. Lebed, Phys. Rev. Lett. **74**, 4603 (1995).

[21] M. C. Arnesen *et al.*, Phys. Rev. Lett. **95**, 071802 (2005).

[22] T. Becher and R. J. Hill, Phys. Lett. B **633**, 61 (2006).

[23] D. Becirevic and A. B. Kaidalov, Phys. Lett. B **478**, 417 (2000).

[24] A. Khodjamirian *et al.*, Phys. Rev. D **80**, 114005 (2009).

[25] S. Di Vita *et al.* (ETM Collaboration), Proc. Sci., LAT2010 (2010) 301.

[26] L. Widhalm *et al.* (Belle Collaboration), Phys. Rev. Lett. **97**, 061804 (2006).

[27] C. T. H. Davies *et al.* (HPQCD Collaboration), Phys. Rev. D **78**, 114507 (2008).

[28] P. Mackenzie (Fermilab Lattice and MILC Collaborations), Proceedings of CKM2010.

[29] J. Koponen *et al.* (HPQCD Collaboration) (work in progress).

[30] For a recent determination of $|V_{cd}|$ and $|V_{cs}|$ from D leptonic decays, see Y. Namekawa *et al.* (PACS-CS Collaboration), Phys. Rev. D **84**, 074505 (2011).